Microstructural Aspects in FSW and TIG Welding of Cast ZE41A Magnesium Alloy

PIERPAOLO CARLONE, ANTONELLO ASTARITA, FELICE RUBINO, and NICOLA PASQUINO

In this paper, magnesium ZE41A alloy plates were butt joined through friction stir welding (FSW) and Tungsten Inert Gas welding processes. Process-induced microstructures were investigated by optical and SEM observations, EDX microanalysis and microhardness measurements. The effect of a post-welded T5 heat treatment on FSW joints was also assessed. Sound joints were produced by means of both techniques. Different elemental distributions and grain sizes were found, whereas microhardness profiles reflect microstructural changes. Post-welding heat treatment did not induce significant alterations in elemental distribution. The FSW-treated joint showed a more homogeneous hardness profile than the as-welded FSW joint.

I. INTRODUCTION

MAGNESIUM alloys are of considerable interest to lightweight structure manufacturing, because of their low density, high specific strength, good thermal conductivity, excellent castability, and fine cutting performance.[1] On the other hand, the scarce corrosion resistance exhibited by most of the Mg alloys, as pointed out by Shi et al.,[2] poses some limits on their wide use. Some issues, related to the poor formability at room temperature and reduced creep resistance of Mg alloys, were remarked by Mordike and Ebert.[3] They argued that the further diffusion of Mg alloys relies on the development of new alloys, the improvement of the manufacturing processes, and the definition of opportune design criteria. In this regard, it has been claimed that the inclusion of well-selected alloying elements leads to a general enhancement of mechanical performance.

Rare earth (RE) elements addition has many advantages, such as purifying alloy melt, modifying castability, refining the microstructure, improving the mechanical properties and anti-oxidation properties. Furthermore, Zirconium addition to RE elements has been shown to improve the mechanical properties due to grain refinement.[4,5] Some studies revealed that the dynamically recrystallized (DRX) grain size of wrought magnesium alloy was lower than that of as-cast magnesium alloy. In addition, the increasing rate of dynamic recrystallization in the as-cast material was considerably lower than the dynamic recrystallization in the wrought material.[6] Lukáč and Trojanová[7] discussed that the addition of rare earth (RE) elements into the material improves its ductility by weakening the basal texture. However, an enhancing of the corrosion rate is also exhibited, as evidenced by Zhao et al.[8] In this regard, recent studies proved the possibility to improve the corrosion resistance of Mg alloys containing RE elements, such as the ZE alloy, by means of heat treatments[9] and Vanadia-based[10] or epoxy-silane coatings.[11]

Mg-Zn-RE alloys, such as the ZE41A alloy, manufactured by casting processes and T5 heat treated, are already successfully employed in the aeronautic and automotive industries. The development of adequate welding processes is considered as a key factor in spreading of Mg alloys for structural application. Tungsten Inert Gas (TIG) and Metal Inert Gas (MIG) processes are widely employed to join Mg alloys using high-purity shielding gases, but several issues still exist. TIG welding of Mg alloys exhibits relatively shallow penetration in single-pass welding and low productivity.[12] Moreover, magnesium melting and solidification, occurring during the conventional welding processes, induce high porosity and weld contamination, compromising the in-service joint performance. In this regard, an increasing interest is currently directed toward the application of the friction stir welding (FSW) process.

To date, effects of RE elements on the microstructure and properties of magnesium alloys have been studied extensively[13,14]; however, very few reports are available in the open literature regarding microstructure evolution in welded material. This paper discusses some experimental results concerning microstructure and metallurgy of ZE41A butt joints welded through both FSW and TIG. Two different temper states of the friction stir

PIERPAOLO CARLONE and NICOLA PASQUINO, Assistant Professors, and FELICE RUBINO, Ph.D. Student, are with the Department of Industrial Engineering, University of Salerno, Fisciano, Italy. Contact e-mail:pcarlone@unisa.it ANTONELLO ASTARITA, Assistant Professor, is with the Department of Chemical Materials and Industrial Production Engineering, University of Naples Federico II, Naples, Italy.

welded joints were investigated, *i.e.*, as-welded and after a post-welding T5 treatment.

II. EXPERIMENTAL

The material under investigation is constituted by Magnesium with the addition of Zinc and RE elements, which are mainly a mixture of Cerium, Lanthanum, Neodymium, and Praseodymium. A certain amount of Zirconium is included in the alloy in order to improve the ductility and the mechanical resistance. ZE41A was manufactured by cast gravity process and supplied in form of strips (with thickness and width equal, respectively, to 4 and 30 mm) by a foundry of the FINMEC-CANICA industrial group. The actual composition of the alloy (wt pct), as obtained by spectrometric analysis, is shown in Figure 1. Aerospace Material Specification SAE AMS 4439F[15] was adopted as reference to assess the acceptability of the samples. The cast material was subjected to a T5 artificial aging treatment at 602 K (29 °C) for 3 hours.

Cast and treated strips were welded in the butt joint configuration, by means of both TIG and FSW welding processes. TIG joints were realized heterogeneously, following the indications of the standard Aerospace Material Specification SAE AMS4392,[16] using an Aerowave Miller AC/DC welding machine. A two-pass welding strategy was adopted to obtain a satisfactory material continuity between the two adjoining edges. Plates were put in contact without a strict control of the gap. The welding torch was equipped with a 7-mm-diameter nozzle provided with a gas lens to laminate the flow of the shielding gas (50 pct Argon and 50 pct Helium high purity mixture). A 3.2-mm-diameter Green (EWPAWSA5.12) electrode was used. The composition of the filler material (W7 welding rod by Magnesium Elektron) was substantially identical to that of the BM. The plates were preheated up to 533 K (260 °C) to reduce the thermal gradient between the BM and the filler, avoiding potential thermal shocks. Welded samples were then polished and finished.
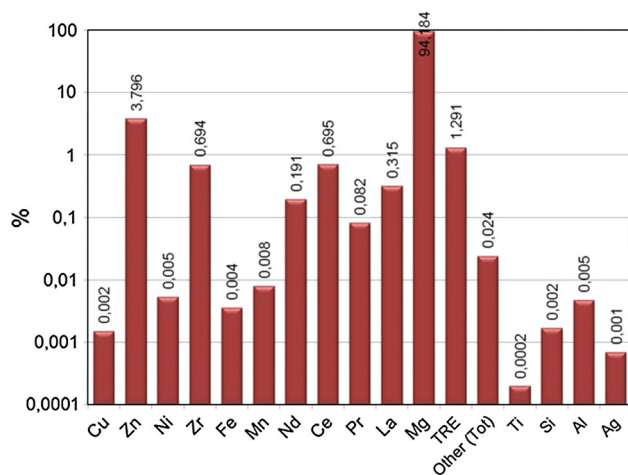
Friction stir welds were executed using a machining center (MCX 600 ECO). The employed tool, realized as a single piece in High Speed Steel, consists of a 20-mm-diameter shoulder with a conical unthreaded pin (height 3.80 mm, major diameter 6.20 mm, and cone angle 30 deg). The processing parameters adopted were the following: rotating speed ω = 1000 rpm; feed rate = 120 mm/minutes; tilt angle = 2 deg; shoulder plunge depth = 0.28 mm. These parameters were chosen according to a previous investigation by some of the authors.[17] A steel clamping fixture was used to fix the material to be welded according to the desired tilt angle. Differently from TIG process, material pre-heating and shielding gas were not employed to execute FSW process. Figure 2 shows the clamping fixture and the tool. No further polishing operation was executed on FSW joint. Summarizing three different samples were studied: (i) TIG joint; (ii) as-welded FSW joint; (iii) FSW T5-treated joint.

Metallurgical specimens, with the main surface perpendicular to the welding direction, were cut away from the welded sheets to observe the microstructure of the weld joint and to perform the microhardness test. Specimens were mounted in a proper thermoset conductive resin and lapped using abrasive disks (320 grade) and subsequently polished with polycrystalline diamond paste (from 9 to 0.05 μm) on tissue disk. Chemical etching, based on a 2.5 pct picric acid solution in ethanol, revealed the microstructure in the different welding zones. The absence of internal defects was checked by optical microscopic analysis. Hitachi TM3000 scanning electron microscope (SEM) was employed to perform high-magnification observations of the weld joints; moreover, electron probe microanalysis (EPMA) was carried out by using an Oxford Instrument Swift ED 3000 probe, equipped with silicon drift detector. The grain size in the welding zones was measured using an image analysis tool and conventional metallographic procedures, according to the standard ASTM E112/E1382.[18] The effect of microstructural alteration on local mechanical properties was investigated by Vickers microhardness tests. A LEICA VMHT-AUTO machine was employed to perform the tests along a programmed linear path. Starting from the mid-thickness of the cross section, tests were executed along five linear patterns (mid line, two lines above and two lines below the mid line) separated each other by 0.5 mm. Other parameters were distance between two consecutive indentations 1 mm, indentation load 100 gf (0.98 N), loading time 15 seconds, indentation speed 60 μm/seconds.

III. RESULTS AND DISCUSSION

High-magnification micrograph of the base material microstructure is given in Figure 3. Fine equiaxed globular grains, rich of precipitates at the boundaries, were detected.

Microscopic investigation of the TIG joint (Figure 4) revealed three different metallurgical zones: a fusion region (FZ) that is made by the material melted during
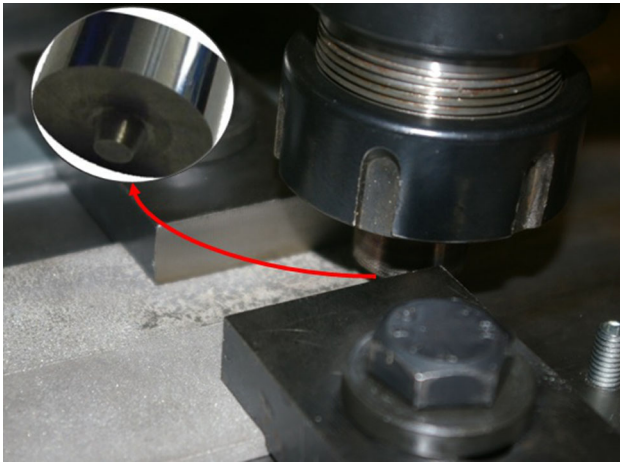

Fig. 1—Composition of the ZE41A Mg alloy.

Fig. 2—Setup and tool for the friction welding process.
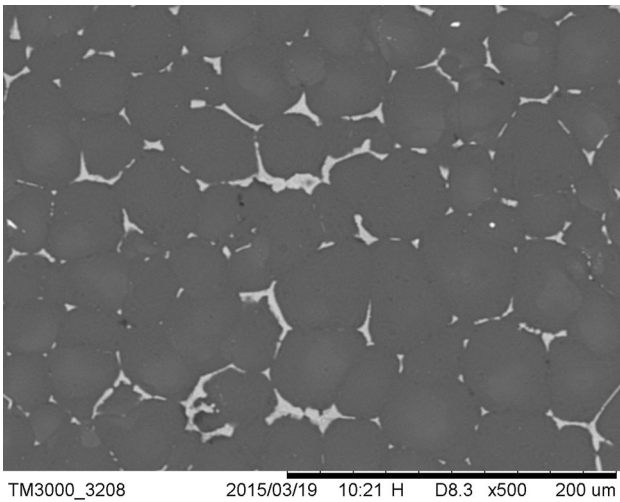
Fig. 3—High-magnification micrographs of base material microstructure.

Fig. 4—High-magnification micrographs of the TIG joint: (*a*) heat-affected zone (HAZ); (*b*) fusion zone (FZ).

the welding and subsequently solidified; a heat-affected zone (HAZ) adjacent to the previous zone; the base material (BM) that was not affected by the welding process.

The microstructure in the FZ (Figure 4(b)) was defined by equiaxed globular grains of smaller dimension (16.3 μm) with respect to the ones of the BM (40.1 μm). This refinement can be attributed to the fast cooling and solidification experienced by the melted material, due to the heat flowing towards the solid zones of the weld. On the other hand, the grains in the HAZ (Figure 4(a)) exhibited a slight increase in size (40.9 μm), reasonably attributable to the grain coarsening promoted at high temperature in the absence of recrystallization phenomena.[19] EDX spectra of the BM and of the welded zone of TIG joint are showed in Figure 5. The grain center appeared rich in Magnesium and Zinc, with atomic percentage close to the eutectic composition of the Mg-Zn system. Conversely, enrichment in other elements, mainly copper and RE, was
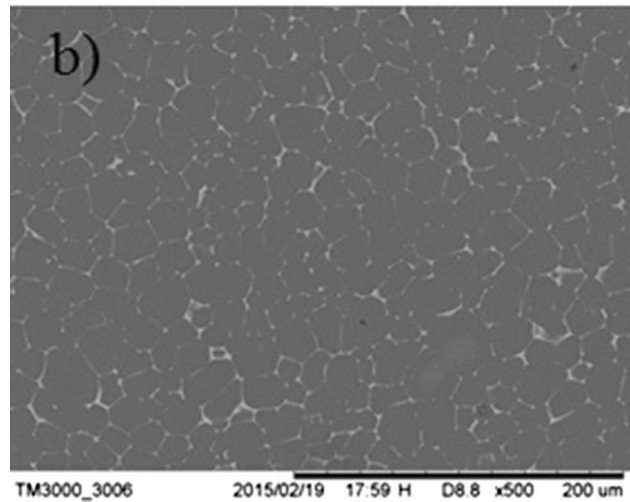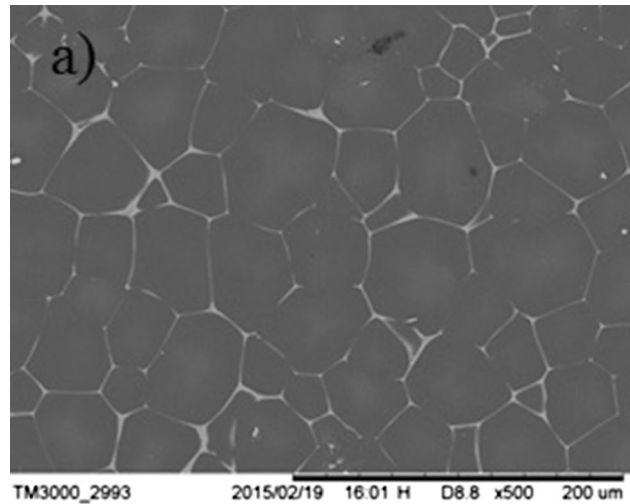
observed at the grain boundary, which appeared very narrow and well defined.

The EDX analysis showed that the distribution of elements in the FZ of the TIG joint approximately reflects what observed for the BM (Figure 5). This is an expected outcome considering the similarity of the thermo-physical history of the material obtained by casting or fusion welding processes. Indeed, microstructure and elemental distribution, in the FZ, were generated by the melting and subsequent cooling and solidification, similarly to what experienced by the base material during the casting process.

Microscopic analysis of a FSW joint (Figures 6 through 9) revealed three main zones, characterized by different crystal grain sizes and shapes.[20] In the core of the bead, namely the nugget zone (NZ), the initial grain and subgrain boundaries were replaced with fine, equiaxed recrystallized grains characterized by a nominal dimension of a few micrometers.

The NZ presented an elliptic shape with onion rings and a distinct flow arm in correspondence of the contact region with the tool shoulder. Fine equiaxed grains (Figure 7) were observed in the NZ, due to continuous
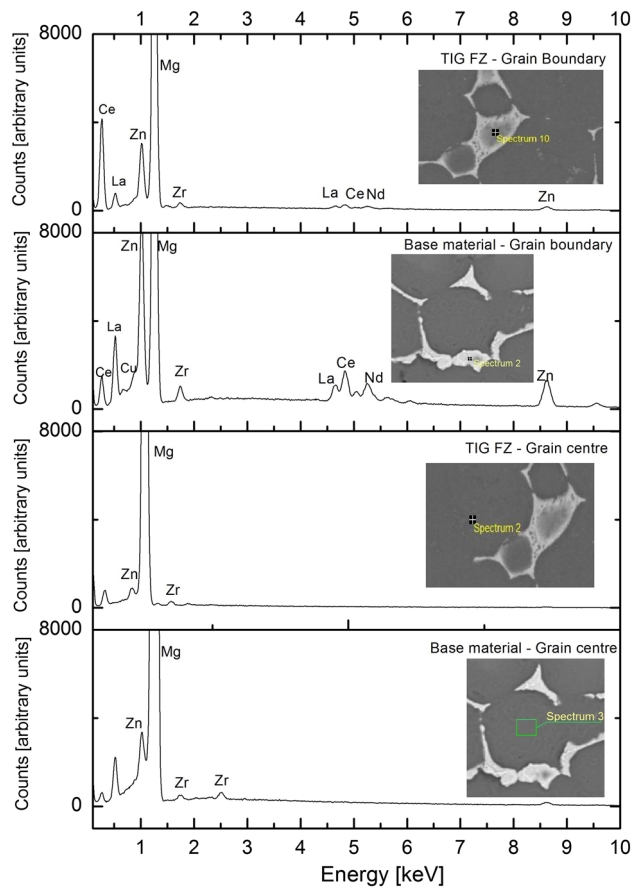
Fig. 5—EDX spectra in the grain center and grain boundary of the BM and FZ of TIG joints.
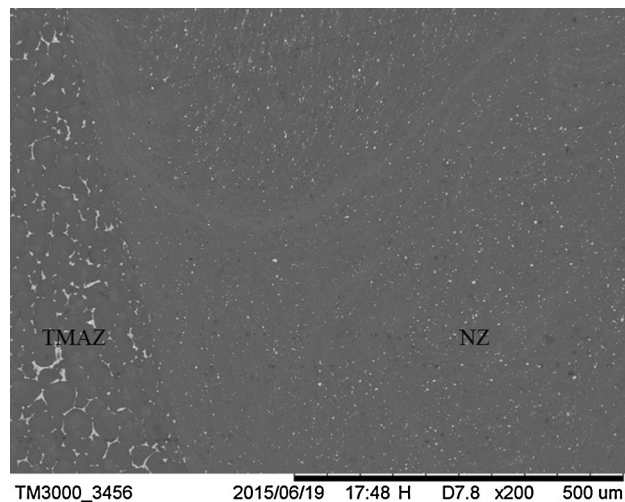

Fig. 6—Macrographs of the as welded FSW specimen, highlighting the transition zone between the NZ and the TMAZ.

dynamic recrystallization phenomena. The grain shape was slightly different with respect to the one of the grains observed in the fused zone of the TIG specimens.[21] This is due to the different formation mechanisms of the grains: in the TIG joints, the grains nucleate and grow from the molten material; conversely in the

nugget zone of the FSW samples the grain structure is due to the dynamic recrystallization phenomena occurring during the welding. The size of the recrystallized grains (9.2 μm) appeared significantly reduced if compared to the base material (BM). A similar grain refinement was reported by Cao and Jahazi[22] relatively to the friction stir processing of sand-cast ZE41A-T5 Mg alloy.

A thermo-mechanical-affected zone (TMAZ), surrounding the NZ, was detected (Figure 8). In this zone, the processing material experienced both the stirring effects promoted by the tool pin and the thermal effects induced by heat generated by friction and plastic dissipation. Consequently, grains were deformed along the flow directions; however, recrystallization phenomena were not as relevant as in the NZ.

Some variations in the appearance of the grain boundaries in the NZ and TMAZ of the FSW joint with respect to the BM were observed. The initial microstructure was constituted by well-defined, regular and narrow separations between adjacent grains, whereas irregular- and less-delineated boundaries were found in welded samples. Such observation was attributed to re-precipitation phenomena occurring after the FSW process. Indeed, precipitate compounds tended to globularization, due to the high temperature and the high deformation experienced. Finally, a heat-affected zone (HAZ), not interested by mechanical stirring but only by thermal phenomena, was observed (Figure 9).

The microstructure of the HAZ appeared qualitatively similar to that of the BM, making the precise identification of such zones quite challenging. In this regard, the inherent complexities of distinguishing HAZ from BM in Mg alloys joined using FSW were already pointed out by some authors.[22] Recent analysis demonstrated that, differently from what accepted for FSW of aluminum alloys, partial recrystallization occurs also in the TMAZ[23] and HAZ[24] of the FSW of some Mg alloys, due to the overcoming of the material recrystallization temperature. This finding was supported by the presence of fine equiaxed grains dispersed between the pancake-elongated grains constituting the initial rolling microstructure. In the present investigation, however, the raw material was characterized by a coarse microstructure with equiaxed grains, because of the gravity cast process and the following T5 heat treatment employed. Consequently, no significant modifications in grains' shape were detected, as highlighted in literature. In the present work, the onset of partial recrystallization phenomena in the TMAZ and HAZ of the FSW joint was supported by the reduction in the grain size, respectively, equal to 23.9 and 34.1 μm, with respect to the BM, due to the presence of redefined small grains. However, in authors' opinion, further work is needed to clarify this aspect.

Figure 10 depicts the EDX spectra in the grain center and at the grain boundary in all metallurgical zones previously described.

As observed for the base material, RE elements tended to precipitate at the grain boundaries. On the other hand, the grain center presented mainly Magnesium and Zinc. A slight presence of Zirconium was
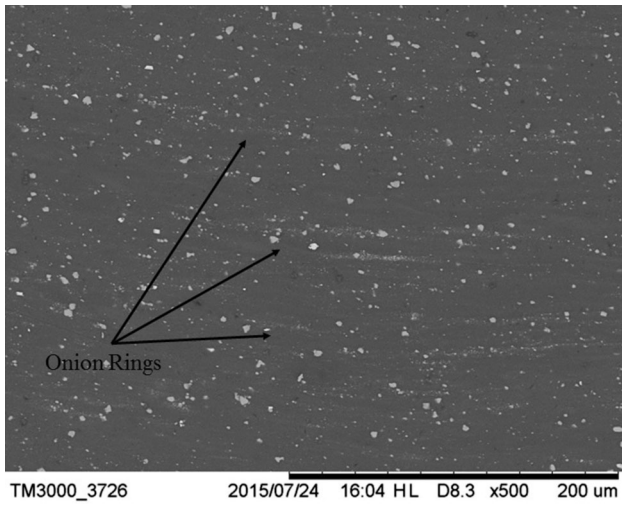
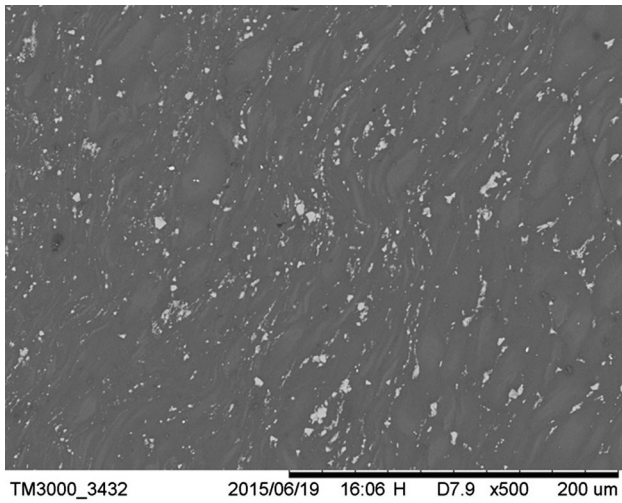Fig. 7—High-magnification micrograph of the nugget zone (as-welded FSW joint).

Fig. 9—High-magnification micrographs of the HAZ in the FSW as-welded joint.

Fig. 8—High-magnification micrograph of TMAZ of the as-welded FSW joint.
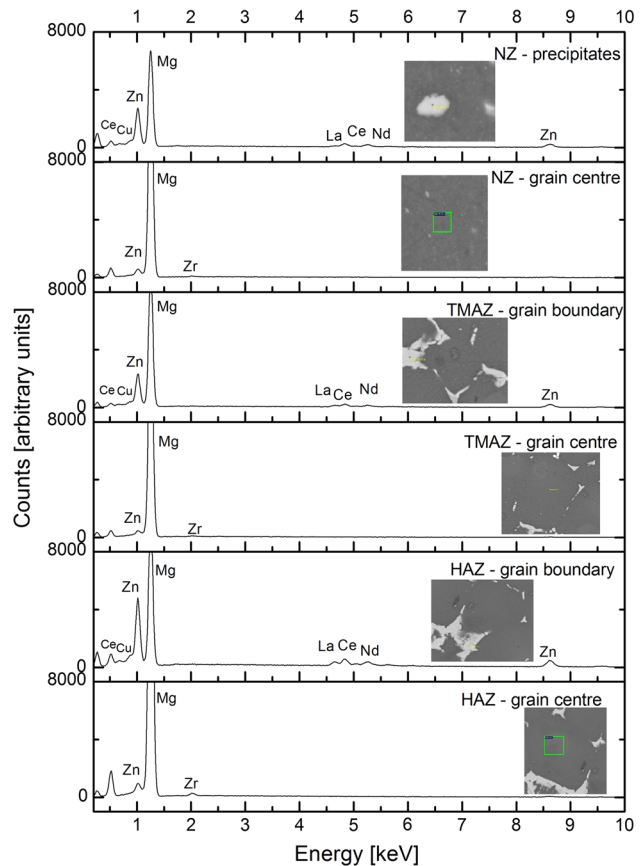
Fig. 10—EDX spectra in the grain center and grain boundary for the as welded FSW joint.

detected in the grain center, probably due to the recrystallization phenomena occurring during the welding. The intensity of the peaks was slightly different if compared to what measured in the BM due to the globularization and re-precipitation phenomena induced by the welding process.

Figure 11 shows high-magnification micrograph of the TMAZ and of the NZ of the FSW joint, re-treated in T5 condition after the welding process. The NZ was interested by a slight coarsening of the grains, with respect to the untreated condition (10.6 μm, with a 13 pct increase, approximately). The main effect of the heat treatment in the NZ was to promote a more homogeneous microstructure. In the TMAZ zone, finer grains attributable to partial recrystallization were observed. What is more, grains appeared less deformed due to globularization phenomena. Intriguingly, the heat treatment significantly affected also the appearance of the grain boundaries, which result narrower and more
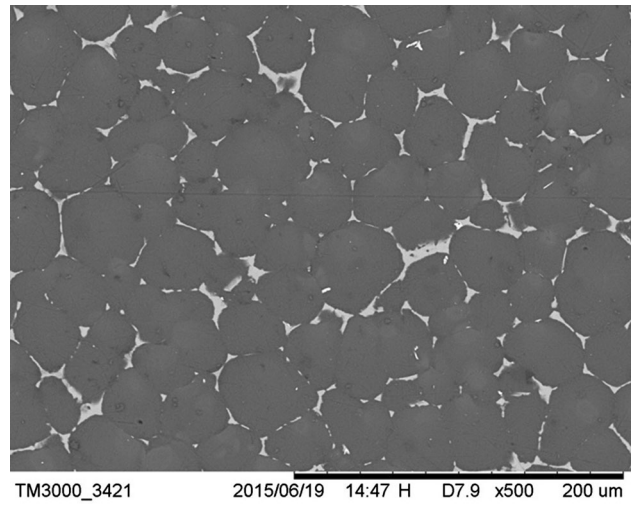
regular and defined. Summarizing after the heat treatment the grain boundaries appeared more similar to the ones of the base material. In both the base material and HAZ, no significant changes were detected.

Figure 12 shows the EDX spectra for the T5-treated FSW sample. As already observed for the untreated
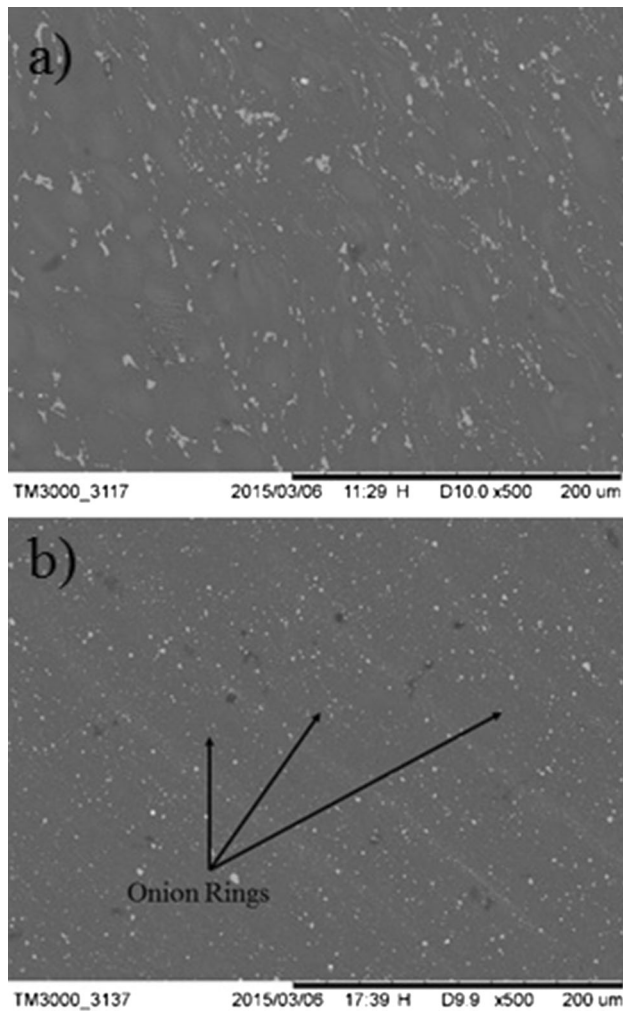
Fig. 11—High-magnification micrographs of the treated FSW joint: (*a*) TMAZ; (*b*) NZ.

Fig. 12—EDX spectra in the grain center and at grain boundary for the T5-treated FSW joint.

sample, the grain center was made mainly by Magnesium and Zinc, whereas grain boundaries were rich of RE elements. Conversely, no Zirconium was detected in the grain center and the measured peaks were more similar to the one of the base materials. The post-welding treatment led to an element distribution and precipitates morphology more similar to the one of the base materials.

Figure 13 shows the microhardness distributions for all the investigated material conditions. Generally speaking, microhardness reflects the microstructural variations induced by the welding processes on the local material properties. Qualitatively similar trends were already described in Mg alloys welded using TIG by Xu et al.[25] and Wang et al.,[15] as well as FSW by Yu et al.[26] Their studies claimed a general reduction of mechanical properties with respect to the base material. In the present investigation, a hardness increase was detected in correspondence of the NZ in FSW joints, attributed to grain refinement and re-precipitation of fine strengthening intermetallic particles (Figure 13(b)).
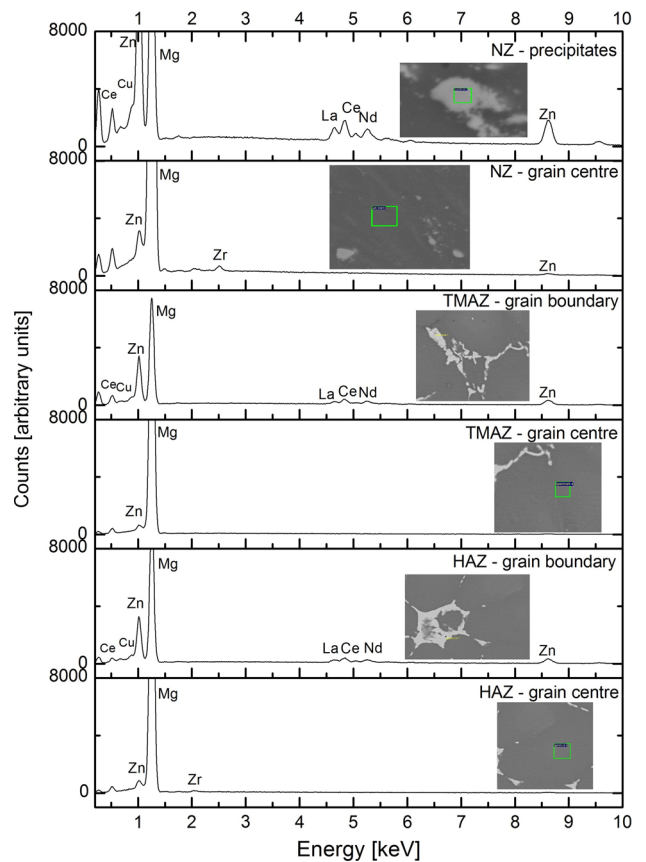
A microhardness reduction was observed in both sides of the NZ. The global minimum resulted lower than the BM value and it is localized in the HAZ, where the structure experienced a softening effect[27] and no strain hardening was induced. Away from the welding center, the microhardness values of the BM were approached.

Analysis of the microhardness profile of TIG joint (Figure 13(a)) disclosed that the microhardness of FZ was lower than what measured in the NZ of FSW joints, consistently with the difference of the grain sizes. The HAZ, induced by the fusion welding process, was wider than the FSW joint, due to the higher temperature (above the melting point) reached by the material with respect to the solid-state stirred material. Additionally, major microhardness reduction in the HAZ of TIG joints was detected, if compared to FSW joints.

FSW-treated joints showed a lower hardness peak in the nugget zone with respect to the as-welded FSW joint, whereas a higher mean hardness was observed in the other zones (HAZ, TMAZ, and BM). Such a result is due to the microstructure homogenization induced by the heat treatment.

IV. CONCLUSIONS

On the basis of the experimental results presented and discussed, the following considerations can be drawn:
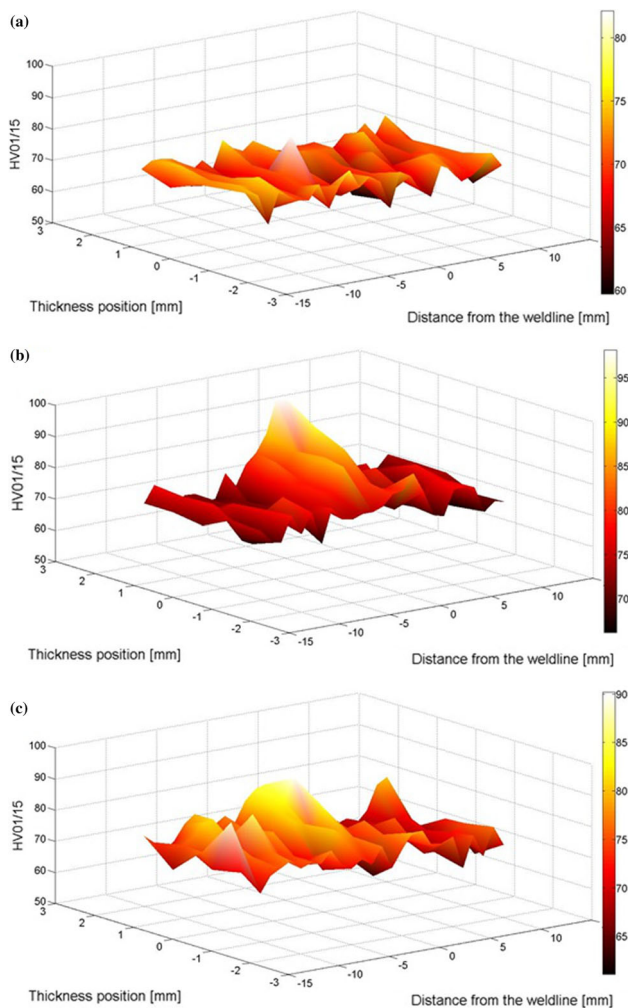
(a)

(b)

(c)

Fig. 13—Microhardness distributions: (*a*) TIG sample; (*b*) FSW as welded sample; (*c*) FSW treated sample.

- The grain boundaries were rich in Rare Earth elements; conversely the grain center was mainly composed by Magnesium and Zinc. The base material microstructure was defined by globular equiaxed grains generated by the treatment experienced.
- In TIG joints, a fusion zone with very small globular grains was observed, produced by the fast cooling experienced by the molten material during the welding process. A heat-affected zone with grains coarsened due to the high temperatures experienced also was detected.
- In FSW joints, the typically observed welding zones (NZ, TMAZ, and HAZ) were detected. NZ was characterized by very fine grains. In the TMAZ deformed grains were observed, whereas refined grains

attributable to partial recrystallization phenomena were individuated in both the TMAZ and HAZ.
- In FSW-T5 joints, a slight grain coarsening with respect to the as-welded joint was detected. Less deformed grains and globularization phenomena occurred on aging were observed in the TMAZ.
- The T5-treated joint disclosed a more uniform hardness distribution if compared to the as-welded joint.

REFERENCES

1. Y.C. Lin, X.M. Chen, Z.H. Liu, and J. Chen: *Int. J. Fatigue*, 2013, vol. 48, pp. 122–32.
2. Z. Shi, G. Song, and A. Atrens: *Corros. Sci.*, 2006, vol. 48, pp. 3531–46.
3. B.L. Mordike and T. Ebert: *Mater. Sci. Eng. A*, 2001, vol. 302 (1), pp. 37–45.
4. G. Ben-Hamu, D. Eliezer, K.S. Shin, and S. Cohen: *J. Alloys Compd.*, 2007, vol. 431, pp. 269–76.
5. Z. Yang, Y.C. Guo, J.P. Li, F. He, F. He, and M.X. Liang: *Mater. Sci. Eng. A*, 2008, vol. 485, pp. 487–91.
6. S.A. Selvan and S. Ramanathan: *Trans. Nonferr. Met. Soc. China*, 2011, vol. 21, pp. 257–64.
7. P. Lukáč and Z. Trojanová: *Mater. Sci. Eng. A*, 2007, vol. 462, pp. 23–28.
8. M.C. Zhao, P. Schmutz, S. Brunner, M. Liu, G. Song, and A Atrens: *Corros. Sci.*, 2009, vol. 51, pp. 1277–92.
9. W.C. Neil, M. Forsyth, P.C. Howlett, C.R. Hutchinson, and B.R.W. Hinton: *Corros. Sci.*, 2001, vol. 53, pp. 3299–308.
10. A.S. Hamdy, I. Doench, and H. Möhwald: *Surf. Coat. Technol.*, 2012, vol. 206, pp. 3686–92.
11. D.K. Ivanou, M. Starykevich, A.D. Lisenkov, M.L. Zheludkevich, H.B. Xue, S.V. Lamaka, and M.G.S. Ferreira: *Corros. Sci.*, 2013, vol. 73, pp. 300–08.
12. L. Wang, J. Shen, and N. Xu: *Mater. Sci. Eng. A*, 2011, vol. 528, pp. 7276–84.
13. L. Gao, R.S. Chen, and E.H. Han: *J. Alloys Compd.*, 2009, vol. 481, pp. 379–84.
14. J.L. Yan, Y.S. Sun, F. Xue, S. Xue, and W.J. Tao: *Mater. Sci. Eng. A*, 2008, vol. 476, pp. 366–71.
15. SAE AMS 4439.
16. SAE AMS 4392.
17. P. Carlone and G.S. Palazzo: *J. Mater. Process. Technol.*, 2015, vol. 215, pp. 87–94.
18. ASTM E112/E1382.
19. S.A. Selvan, S. Ramanathan, R. Karthikeyan, and B.K. Raghunath: *Trans. Nonferr. Met. Soc. China*, 2010, vol. 20 (1), pp. 22–27.
20. J. Su, T.W. Nelson, and C.J. Sterling: *Mater. Sci. Eng. A*, 2005, vol. 405 (1–2), pp. 277–86.
21. A. Squillace, A. De Fenzo, G. Giorleo, and F. Bellucci: *J. Mater. Process. Technol.*, 2004, vol. 152, pp. 97–105.
22. X. Cao and M. Jahazi: *Proceedings of the 46th Annual Conf. of Metallurgists of CIM*. 1 st ed., M.O. Pekguleryuz, Toronto, Canada, 2007, pp. 169–80.
23. N. Afrin, D.L. Chen, X. Cao, and M. Jahazi: *Mater. Sci. Eng. A*, 2008, vol. 472, pp. 179–86.
24. S.M. Chowdhury, D.L. Chen, S.D. Bhole, and X. Cao: *Mater. Sci. Eng. A*, 2010, vol. 527, pp. 6064–75.
25. N. Xu, J. Shen, W. Xie, L. Wang, D. Wang, and D. Min: *Mater. Charact.*, 2010, vol. 61, pp. 713–19.
26. S. Yu, X. Chen, Z. Huang, and Y. Liu: *J. Rare Earths*, 2010, vol. 28 (2), pp. 316–20.
27. X. Cao, M. Xiao, M. Jahazi, and J.-P. Immarigeon: *Mater. Manuf. Process.*, 2005, vol. 20, pp. 987–1004.